International Journal of Nanoelectronics and Materials
Volume 13, No. 3, July 2020 [537-546]

Synthesis of Chicken Eggshell Based Nanofluorapatite Using Sonochemical and Microwave-Assisted Precipitation Methods

Kiagus Dahlan[1,2,*], Yessie Widya Sari[1], Nur Aisyah Nuzulia[1], Dina Yauma Asra[1], Zudah Sima'atul Kubro[2], Miftakhul Hasan[1] and Muhammad Fakry Alrasyid[1]

[1]*Division of Biophysics, Department of Physics, Bogor Agricultural University, Bogor, Indonesia 16680.*
[2] *Advanced Research Laboratory, Bogor Agricultural University, Bogor, Indonesia 16680.*

Received 23 February 2020, Revised 14 July 2020, Accepted 18 August 2020

ABSTRACT

Fluorapatite ($Ca_{10}(PO_4)_6F_2$) is a fluorinated calcium phosphate that has high chemical and structural stability. Therefore, it is suitable to cover the outer layer of teeth. A variety of methods and synthetic chemicals have been used to produce fluorapatite. This paper reports the synthesis of nanofluorapatite using sonochemical and precipitation methods with chicken eggshells were used as the natural sources of calcium. The synthesis was also assisted by microwave irradiation, after precipitation processes, to be more efficient and faster. The irradiation was applied at a microwave power of 200 W and 400 W for 30 minutes and 45 minutes, respectively. The effect of ultrasonication amplitude was also observed in this experiment. Two different amplitudes applied are 20% and 40% of the maximum. The results reveal that accurate composition of CaO, H_3PO_4, and NH_4F are needed to obtain pure chicken eggshell based fluorapatite as presented by X-ray diffractometer. This result is supported by Fourier Transform Infrared Spectrophotometer (FTIR) showing the presence of fluorapatite functional groups. Scanning Electron Microscope (SEM) with Energy-dispersive X-ray (EDX) spectroscopy was used to evaluate the surface morphology of the samples and the elements present near the surface. The scanning spectroscopy shows that the samples contained the elements of fluorapatite which are C, Ca, O, P and F. It was also presented by the microscope that the average particle sizes at a point were in the range of 68-117 nm, polygonal in shape and agglomerates.

Keywords: Bioceramics, Fluorapatite, Precipitation, Ultrasonication.

1. INTRODUCTION

Calcium phosphate or calcium apatite is a bioceramic that has extensive application in the healing processes of bones and teeth due to its biocompatibility and similar composition to that of natural bones. It also functions as the main source of inorganic phosphor in nature. Hydroxyapatite, $Ca_{10}(PO_4)_6(OH)_2$, is one of the calcium phosphates phases that has been studied by many researchers [1-5]. However, hydroxyapatite has low structural and chemical stability and, therefore, very quickly dissolved in body fluid. In order to obtain more stable bioceramics, fluorapatite is developed [6-13]. Fluorapatite is formed by substituting OH^- functional groups in hydroxyapatite with F^- ions. The substitution gives greater structural stability of the fluorapatite since fluorine is the most electronegative chemical element and F^- has closer coordination to the nearest calcium than the hydroxyl.

Fluorapatite, $Ca_{10}(PO_4)_6F_2$, has chemical compositions, biocompatibility, and bioresorbability that are equivalent to inorganic matrices for bones and teeth. Fluorapatite forms the outer layer of

*Corresponding Author: *kdahlan@apps.ipb.ac.id*

teeth as it has higher chemical and structural stability and ability to form the acid-resistant structure in tooth enamel [14-16]. The structure of fluorapatite consists of PO_4^{3-}tetrahedra which is similar to trees forming a hexagonal axis with F- ions along its axis [17]. The exchange of F- ions with other mineral apatite is influenced by nature which depends on its size. The smaller the particle size available, the better will be the adsorption capacity of the fluoride.

Nanofluorapatite or nanosized fluorapatite (n-FA) can be produced by various methods of synthesis including sonochemical and precipitation assisted with microwave irradiation methods. The sonochemical method applies ultrasound to speed up the chemical reaction and increase in reaction output and, therefore, may reveal faster and more specific chemical reactions. This method could also result in nanosized particles [18-20]. Precipitation method is mostly used because the method is very simple [15,21]. Recently, many researchers combined this method with microwave irradiation. Microwave which has a frequency of about 2.45 GHz may provide shorter synthesis time and save a lot of energy [22-28]. The wave at this frequency provides electromagnetic energy that can be absorbed by water and lipid molecules and, thus, intensifies molecular interactions in the solution [29].

The main component of fluorapatite is calcium. Synthetic calcium nitrates are mostly used as the calcium precursor in fluorapatite synthesis [16, 30-32]. Various non-synthetic materials such as seashells and chicken eggshells can be used. Chicken eggshells contain more than 90 per cent calcium carbonate and, therefore, this agricultural waste could be used as the calcium precursor [33]. The use of a large number of chicken eggshells in producing calcium phosphate compounds may contribute to saving clean environments. Moreover, using biological sources as starting materials could induce better bioactive and biocompatible products.

This research aimed to synthesize chicken eggshell based nanofluorapatite using sonochemical and microwave-assisted precipitation methods. Variation in the concentration ratio of starting materials was performed to study its effect on the impurities of the resulted fluorapatite. So, the variation in ultrasonication amplitudes was also recorded to observe its effect on the crystallinity and particle size of fluorapatite powder. Effect of variation in microwave power was also investigated.

2. EXPERIMENTAL SECTION

Chicken eggshells, H_3PO_4 and NH_4F compounds were used as starting materials. Chicken eggshells were firstly washed to remove macro dirt and unwanted materials. The cleaned chicken eggshells were then calcined using a furnace at 1000°C for 5 hours to remove the organic components. Calcination processes may release CO_2 from $CaCO_3$ as the major component of chicken eggshells and produce CaO [34]. To determine the calcium content in chicken eggshells, after calcination processes, the samples were examined by using atomic absorption spectrometer (AAS). The resulted CaO was then grounded to fine powder using mortar and pestle. The mass of chicken eggshells, the resulted CaO and fluorapatite powders were weighed.

Stoichiometric mole ratios in fluorapatite synthesis for C:P and P:F is 1.67:1 and 3:1, respectively. Two different molarities of starting materials were used in this experiment. Fluorapatite was synthesized by firstly mixing phosphoric acid solution and NH_4F solution to obtain phosphorus-fluoride precursor solution [35-36]. This mixture was then slowly added to 100 ml aqueous calcium oxide suspension. Magnetic stirring was applied during the mixing processes. Another route of synthesis was also performed by adding NH_4F powders into hydroxyapatite that has been synthesized earlier in an aqueous environment [37-38].

Furthermore, the sample was irradiated in a microwave oven. The use of microwave irradiation aimed to replace the ageing processes that usually takes 24 hours or more in the synthesis of

calcium phosphate bioceramics. Microwave irradiation applied was at a power of 200 W and 400 W for a duration of 30 minutes and 45 minutes. Sintering processes were performed afterwards for 2 hours at a temperature of 600°C with a rise of 5°C/minute. After irradiation was completed, the sample was then mashed and stored in a desiccator. The sonochemical method with maximum ultrasonication amplitudes of 20% and 40% was applied during precipitation processes.

X-ray diffraction (XRD) characterization was employed to determine the phase purity and the crystallinity of the resulted powders using Shimadzu X-ray Diffractometer equipped with a Cu-Kα radiation, 40 kV, 30 mA rotating anode. The diffraction patterns were collected at room temperature over an angular range of 10° to 80° with 0.02° step size and a scan speed of 2°/min. Phase identification was obtained by comparing diffraction patterns of the resulted samples with fluorapatite patterns in Joint Committee on Powder Diffraction Standard (JCPDS) database.

Samples were also characterized by Fourier Transform Infrared (FTIR) spectrometer ABB MB 3000 to identify the phase and the functional groups of the samples. The characterization was performed by mixing 2 mg of sample powder with 100 g potassium bromide (KBr) to form a pellet which was then measured by FTIR spectrophotometer with a wavenumber range of 400-4000 cm^{-1}. To observe the surface morphology of the samples and the elements present near the surface, a scanning electron microscope with energy dispersive X-ray (SEM: JEOL JSM-360LA) spectroscopy was used. Figure 1 shows the flow chart of the experimental procedures.

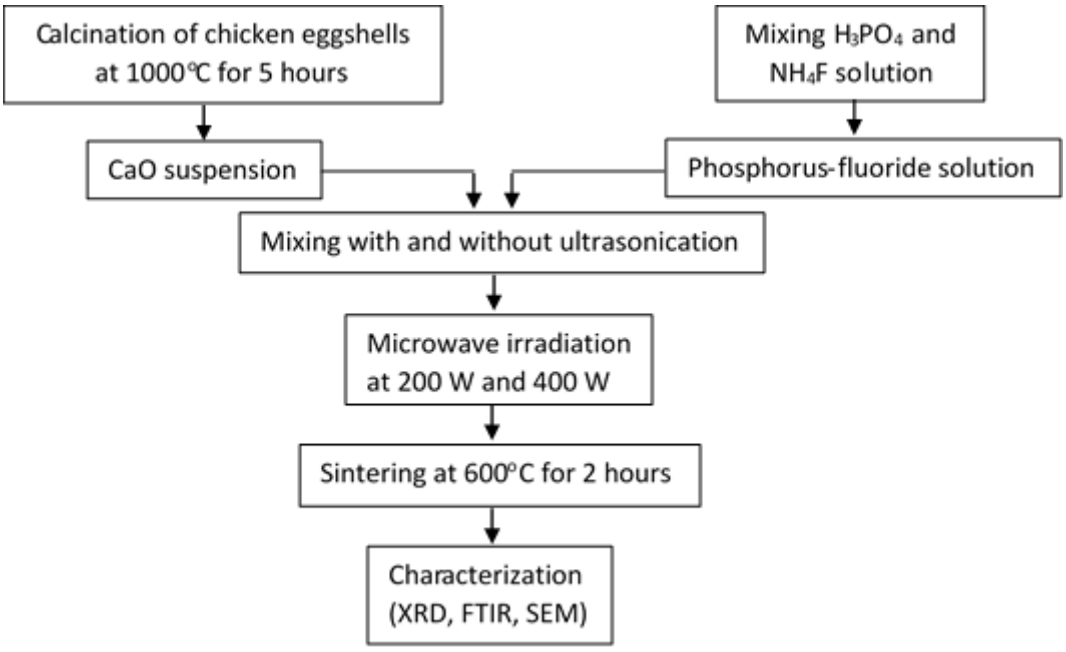

Figure 1. Flow chart of fluorapatite synthesis.

3. RESULTS AND DISCUSSION

3.1. Calcination and Synthesis Results

Mass of chicken eggshells was weighed before and after calcination. It reduced up to about 55% after calcination. It means 1 kg of chicken eggshells may produce about 550 g CaO. CaO was the decomposition product of $CaCO_3$ due to the high-temperature firing during calcination processes (1000°C for 5 hours) which releases the carbon compounds. The average percentage of calcium in CaO powder, measured with atomic absorption spectrophotometer (AAS), was about 63.2%. Hence, indicating the high potential amount of CaO stored in this organic waste.

Table 1 presents molarity of the starting materials and the mass of the resulted fluorapatite powder. The experiments were performed with ultrasonication and without ultrasonication. The results show that the ultrasonication did not make any effects on the number of powders collected. Utrasonication may affect the time of reaction because of its function to speed up the interaction between the reactants. Two different molarities with the same mole ratio were used. The results, as shown by Table 1, present that the number of fluorapatite powder resulted was proportional to the molarities of the starting materials.

Table 1 Ultrasonication amplitude and molarity of starting materials

Ultrasonication amplitude (%)	Molarity of starting materials (M) in 100 ml distilled water			Mass of resulted powder (g)
	CaO	H_3PO_4	NH_4F	
0	1.67	1.00	0.33	14.47± 0.25
	0.50	0.30	0.10	3.70 ± 0.12
20	1.67	1.00	0.33	14.28 ± 0.26
	0.50	0.30	0.10	3.86 ± 0.14
40	1.67	1.00	0.33	14.53 ± 0.24
	0.50	0.30	0.10	3.82 ± 0.12

3.2. Phase Structure Analysis

Figure 2 shows the XRD patterns of fluorapatite resulted from precipitation with microwave assistance method by mixing CaO, H_3PO_4 and NH_4F solution and sintering the result at a temperature of 600°C. It can be seen from the figure that this method results in pure fluorapatite. The highest peak is at 31.98° as also found in JCPDS database No. 150876. This pure fluorapatite was also obtained when fluorapatite was synthesized by adding NH_4F powder into hydroxyapatite that has been synthesized earlier. The XRD patterns found by implementing the sonochemical method also present pure fluorapatite.

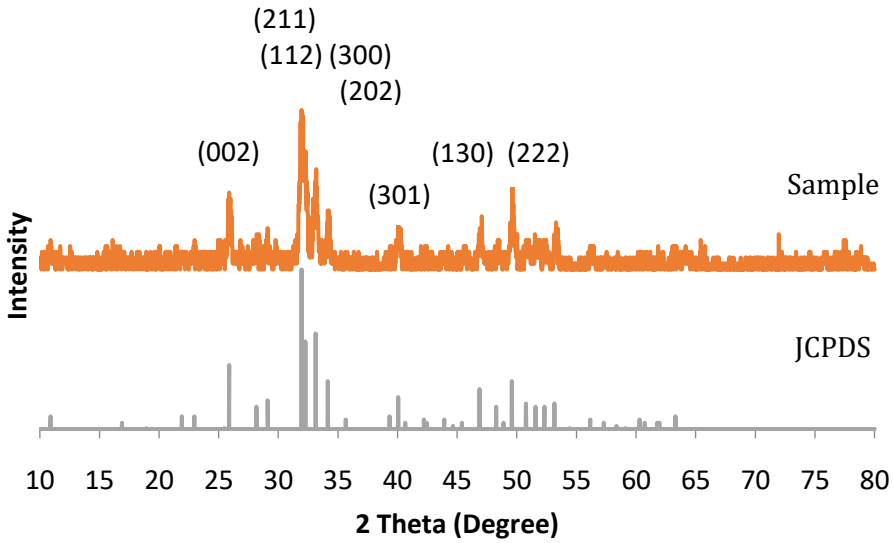

Figure 2. XRD patterns of pure fluorapatite sample obtained from the experiment (above), and JCPDS database (below). Samples resulted from microwave-assisted precipitation synthesis by mixing CaO, H_3PO_4 and NH_4F solution and sintering the result at a temperature of 600°C. Similar patterns were also found for fluorapatite synthesis using the sonochemical method.

Figure 3 shows the XRD patterns from samples synthesized using lower molarity of starting materials. 50 ml solution of 1 M H_3PO_4 was mixed with 50 ml solution of 0.33 M NH_4F. This mixing reduces the molarity of each solution twice. Thus, when this mixture is combined with CaO in 100

ml distilled water, the number of CaO particles are not comparable with the number of H_3PO_4 and NH_4F particles in the solution. Therefore, it can be seen from Figure 3 that there are peaks that do not belong to fluorapatite. These peaks at the angle 18.09° belong to $Ca(OH)_2$ (JCPDS database No. 04-0733) and at angles of 37.54° and 37.48° belong to CaO (JCPDS database No. 37-1497). This figure shows the patterns of samples resulted from precipitation method with sonication and without sonication. $Ca(OH)_2$ and CaO peaks arise may be due to some of the CaO particles are not involved in the reaction due to the lack of H_3PO_4 and NH_4F particles. Similar phenomena were also observed in the synthesis of carbonated hydroxyapatite (CHA) in which carbonate level in CHA powder increased with the increasing of CO_3^{2-}/PO_4^{3-} ratio [36, 39-40]. However, by applying ultrasonication, the intensity of $Ca(OH)_2$ and CaO decreased without decreasing the intensity of peaks of fluorapatite. This result proves that ultrasonication increases the reaction output. Figure 3 also indicates that to get a pure fluorapatite phase, a precise mole ratio of the starting materials is needed [37, 41].

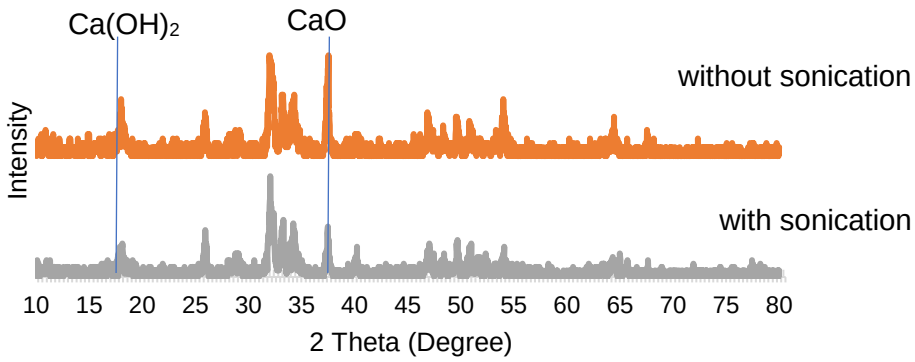

Figure 3. XRD Patterns of samples without sonication (above) and samples with sonication (below).

3.3. Crystallinity and Lattice Parameters

Effect of ultrasonication amplitude in crystallinity of the samples was also observed in this experiment. Two different amplitudes were applied, 20% and 40%. As the ultrasound was applied, the crystallinity increased from 81.73% to 85.61%. Ultrasonication amplitudes as seen in Table 2 slightly affect the crystallinity of the samples, although statistically insignificant. Crystallite size of the samples is found in the range of 35.4 nm and 43.5 nm and is not influenced by the ultrasonication amplitudes.

Table 2 The crystallinity of the samples

Ultrasonication Amplitude (%)	Crystallinity (%)
0	81.73
20	85.61
40	88.95

Lattice parameters were obtained by calculations using the Cohen method. The calculation results for lattice parameters of the fluorapatite powders reveal the lattice parameters for a = b = 9.370 Å and c = 6.860 Å, and these values are very close to the fluorapatite lattice parameter values on JCPDS which are a = b = 9.368 Å and c = 6.884 Å. Therefore, it might be concluded that all samples belong to the category of fluorapatite hexagonal crystal structure. The average accuracy of lattice parameters obtained is 99.33% for lattice parameters a = b and 99.07% for lattice parameters c.

3.4. Functional Groups and Surface Morphology

FTIR spectroscopy identifies the functional groups and may show the process of fluorine substitution. Based on the FTIR characterization results shown in Figure 4, the overall results of the experiment show the presence of functional groups that approach the values of fluorapatite obtained elsewhere [32].

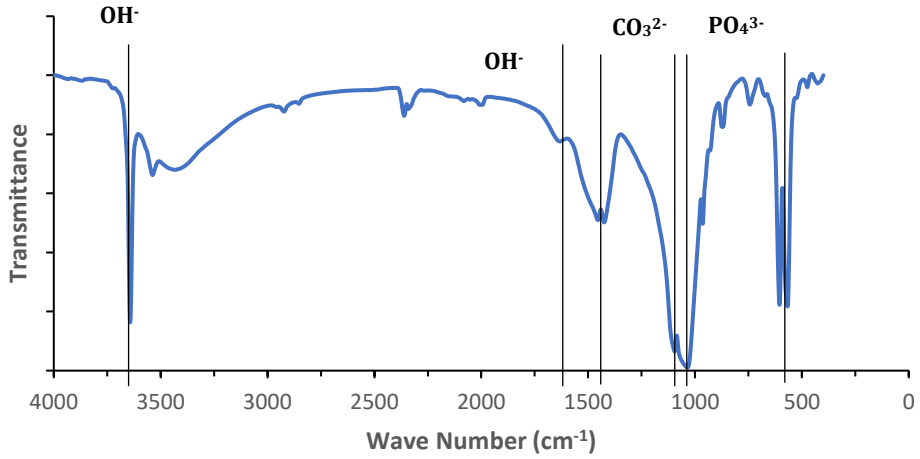

Figure 4. FTIR spectra of fluorapatite.

The PO_4^{3-} functional group has four vibration modes, namely symmetric stretching (ν_1), symmetric bending (ν_2), asymmetric stretching (ν_3), and asymmetric bending (ν_4). The four vibrations are present in Figure 4 at the wavenumbers of 963.96 cm^{-1}, 474.66 cm^{-1}, 1035.24 - 1095.78 cm^{-1}, and 567.06 - 604.53 cm^{-1}, respectively. Figure 4 also shows asymmetric stretching (ν_3) of CO_3^{2-} functional group found at wavenumbers of 1424.86 cm^{-1} and 1454.47 cm^{-1}. OH^- functional group with vibration asymmetry stretching (ν_3) also can be seen at wavenumbers of 2923.14 cm^{-1} and 3434.52 cm^{-1}. The presence of FHOOHF- (ν) functional group at the wavenumber of 743.18 cm^{-1} indicates that the system has completely changed OH^- functional groups with F^- ions [32]. At the wavenumber of 1420 cm^{-1}, Figure 4 shows the presence of carbonate functional group appeared in the samples. This is possible due to carbon dioxide contamination from the atmosphere.

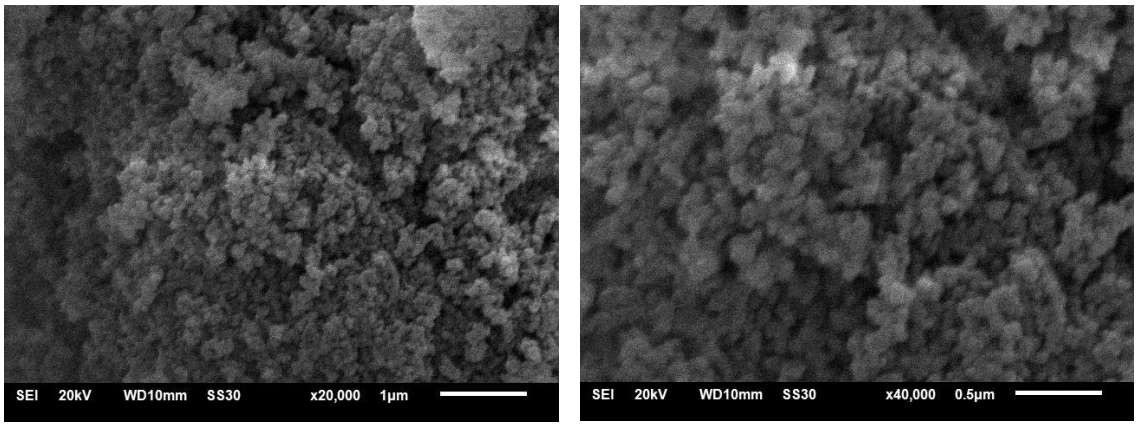

a) b)

Figure 5. Scanning electron micrographs at a magnification of a) 20,000 times, and b) 40,000 times. The morphology looks very similar, so is also the particle sizes, even though the irradiation times were different. Samples: a) using microwave power of 200 W for 30 minutes, and b) using microwave power of 200 W for 45 minutes.

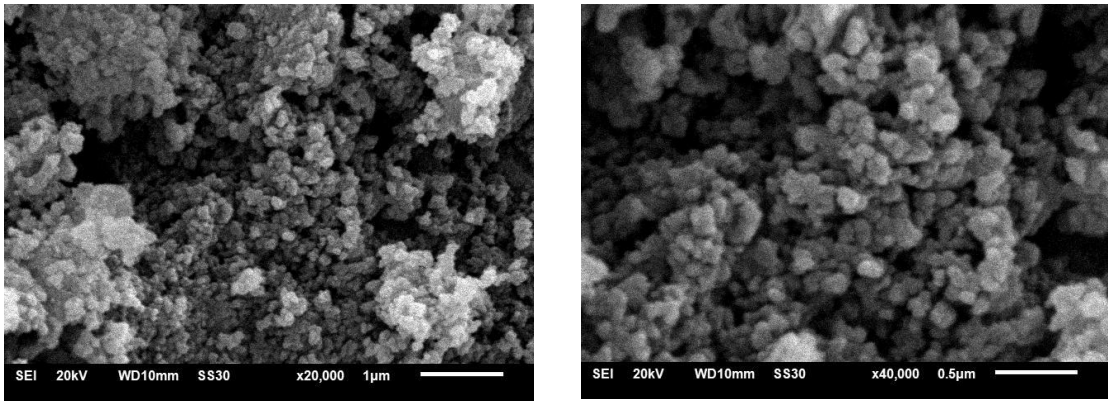

a) b)

Figure 6. Scanning electron micrographs at a magnification of a) 20,000 times, and b) 40,000 times of samples irradiated in a microwave oven of 400 W for 45 minutes.

Scanning electron microscope observations of the obtained powders are presented in Figures 5 and 6. SEM images show similarities in surface morphology of the whole samples which is a polygonal shape and has many clumps. SEM did not observe the difference in shapes between samples. Figure 5a shows SEM image with a magnification of 20,000 times of sample resulted from microwave irradiation power of 200 and irradiation time of 30 minutes, while Figure 5b shows SEM image with a magnification of 40,000 times of sample resulted from microwave irradiation power of 200 and irradiation time of 45 minutes. The shapes of particles look very similar which are polygonal and agglomerated. Figure 6 shows SEM images of samples resulted from microwave irradiation power of 400 W for 45 minutes with a magnification of 20,000 times (Figure 6a) and 40,000 times (Figure 6b).

The particle size of the fluorapatite powders ranges from 68 nm to 117 nm. There is no significant difference obtained between samples synthesized by using microwave irradiation time of 30 minutes and 45 minutes. However, a slight difference was observed on particle size from samples with microwave powers of 200 W and 400 W which are 90.2 nm and 80.1 nm, respectively. The results of EDX characterization in samples show the presence of several detected elements, which are C, O, P, Ca, and F as shown in Table 3. It can be seen that ultrasonication reduces the number of carbons from 21.41% (untreated) to 7.54% (treated) which means reducing carbonate groups in samples.

Table 4 Mass percentage of elements in powder samples

Mass (%)	Ultrasonication Treatment	
	Untreated	Treated
Ca	24.26	32.98
P	3.5	7.42
F	2.24	2.98
O	48.18	48.72
C	21.41	7.54

4. CONCLUSION

Nanofluorapatite was successfully synthesized by using chicken eggshells as the calcium precursor. The synthesis used sonochemical and precipitation methods with microwave irradiation assistance. Pure fluorapatite was obtained as presented by XRD patterns. Crystallinity increased from 81.73% to 85.61% as the ultrasonication was applied. Two different amplitudes of ultrasonication were applied, 20% and 40%, which reduces the impurity of the samples. Crystallite size of the samples is found to be in the range of 35.4 and 43.5 nm.

SEM images show similarities in surface morphology of the whole samples which is the polygonal shape and has many clumps. The particle size of the fluorapatite samples ranges from 68 nm to 117 nm. There is no significant difference in particle sizes obtained between samples resulted from microwave powers of 200 W and 400 W, and between microwave irradiation time of 30 minutes and 45 minutes. The results of EDX characterization in samples show the presence of several detected fluorapatite elements, which are C, O, P, Ca, and F.

This research proved that chicken eggshells may be used as calcium precursor to produce nanosized pure fluorapatite. The use of natural source could induce better bioactivity and biocompatibility. Chicken eggshell based fluorapatite also has good crystallinity, morphology, and small particle size which is an advantage to result in better cellular response.

REFERENCES

[1] Ferraris, S., Yamaguchi, S., Barbani, N., Cazzolaa, M., Cristallini, C., Miolaa, M., Vernèa, E. & Sprianoa, S. Bioactive materials: In vitro investigation of different mechanisms of hydroxyapatite precipitation. Acta Biomaterialia **102** (2020) 468–480.

[2] Okuda, K., Hirota, K., Mizutani, T. & Aoyama, Y. Co-precipitation of tapioca starch and hydroxyapatite: Effects of phosphorylation of starch on mechanical properties of the composites. Results in Materials **3** (2019) 100035.

[3] Dahlan, K., Nuzulia, N. A., Wahyudi, S. T. & Utami, S. Effect of Na Alginate in the porosity of scaffolds of byphasic calcium phosphate/alginate composites. Key Engineering Material **696** (2016) 183-186.

[4] Wahyudi, S. T. *et al.* Simple and easy method to synthesize chicken eggshell-based hydroxyapatite. Advanced Materials Research **896** (2014) 276-279.

[5] Noviana, D. *et al.* In vivo study of hydroxyapatite-chitosan and hydroxyapatite-tricalcium phosphate bone graft in sheep's bone as animal model. Proceedings-2nd International Conference on Instrumentation, Communication, Information Technology, and Biomedical Engineering, (2011) 403-408.

[6] Montazeri, N., Jahandideh, R. & Biazar, E. Synthesis of fluorapatite-hydroxyapatite nanoparticles and toxicity investigations. International Journal of Nanomedicine **6** (2011) 197–201.

[7] Shafiei, F., Behroozibakhsh, M., Moztarzadeh, F., Haghbin-Nazarpak, M & Tahriri, M. Nanocrystalline fluorine-substituted hydroxyapatite $[Ca_5(PO_4)_3(OH)_{12x}F_x$ $(0 \leq x \leq 1)]$ for biomedical applications: preparation and characterisation. Micro & Nano Letters **7**, 2, (2012) 109-114

[8] Kevin J. Roche, Kenneth T. Stanton. Measurement of fluoride substitution in precipitated fluorhydroxyapatite nanoparticles. Journal of Fluorine Chemistry. 2014.161, 102-109

[9] Jokanović, V., Colović, B., Sandić-Živković, M., Bajić, M. P. & Živković, S. Structural characteristics and mechanisms of fluorapatite mechanochemical synthesis. Serbian Dental Journal **63** (2016) 74-80.

[10] Kubro, Z. S., Wahyudi, S. T. & Dahlan, K. Synthesis of calcium phosphate: influence of sintering temperature on the formation of fluorhydroxyapatite. International Journal of Nanoelectronics and Materials **13** (2020) 63-70.

[11] Švarc-Gajić J. *et al.* Determination of fluorides in pharmaceutical products for oral hygiene. Journal of Food and Drug Analysis **21** (2013) 384–389.
[12] Wei, W., Wang, X., Wang, Y., Xu, M., Cui, J. & Wei, Z. Evaluation of removal efficiency of fluoride from aqueous solution using nanosized fluorapatite. Desalination and Water Treatment **52** (2014) 31-33.
[13] Kirboga, S., Oner, M. & Akyol, E. The effect of ultrasonication on calcium carbonate crystallization in the presence of biopolymer. Journal of Crystal Growth **401** (2014) 266–270.
[14] Kim, H. W., Kim, H. E. & Knowles, J. C. Fluor-hydroxyapatite sol-gel coating on titanium substrate for hard tissue implants. Biomaterials **25** (2004) 3351-3358.
[15] Ghomi, F., Jalilifiroozinezhad, S. & Azami, M. New precipitation method for synthesis of nano-fluorapatite. Materials Research Innovations **17** (2013) 257-262.
[16] Sasani, N., Ayask, H. K., Zebarjad, S. M. & Khaki, J. V. Characterization of rod-like high-purity fluorapatite nanopowders obtained by sol-gel method. Journal of Ultrafine Grained and Nanostructured Materials **46** (2013) 31-37.
[17] Vassilikou-dova, A., Macalik, B., Kalogeras, I. M., Calamiotou, M., Londos, C. A. & Fytros, L. TSDC probe of anisotropic polarizability in fluorapatite single crystals. Radiation Effects and Defects in Solids **149** (1999) 279-286.
[18] Bang, J. H. & Suslick, K. S. Applications of ultrasound to the synthesis of nanostructured materials. Advanced Materials **22** (2010) 1039-1059
[19] Xu, H., Zeiger, B. W. & Suslick, K. S. Sonochemical synthesis of nanomaterials. Chemical Society Review **42** (2013) 2555-2567.
[20] Brundavanam, S., Poinern, G. E. J. & Fawcett, D. Synthesis of a hydroxyapatite nanopowder via ultrasound irradiation from calcium hydroxide powder for potential biomedical application. Nanoscience and Nanoengineering **3** (2015) 1-7.
[21] Yelten-Yilmaz, A. & Yilmaz, S. Wet chemical precipitation synthesis of hydroxyapatite (HA) powders. Ceramics International 44 (2018) 9703-9710.
[22] Kumar T. S. S., Manjubala, I. & Gunasekaran, J. Synthesis of carbonated calcium phosphate ceramics using microwave irradiation. Biomaterial **21** (2000) 1623-1629.
[23] Hassan, M. N., Mahmoud, M. M., El-Fattah, A. A. & Kandil, S. Microwave-assisted preparation of Nano-hydroxyapatite for bone substitutes. Ceramics International **42** (2016) 3725-3744.
[24] Sajahan, N. A. & Wan Ibrahim, W. M. A. Microwave irradiation of nano-hydroxyapatite from chicken eggshells and duck eggshells. The Scientific World Journal (2014) 1-7.
[25] Shah, J. J. & Mohanraj, K. Comparison of conventional and microwave-assisted synthesis of benzotriazole derivatives. Indian Journal of Pharmaceutical Science **76** (2014) 46-53.
[26] Asra, D. Y., Sari, Y. W. &, Dahlan, K. Effect of microwave irradiation on the synthesis of carbonated hydroxyapatite (CHA) from chicken eggshell. IOP Conference Series: Earth and Environmental Science **187** (2018) 012016.
[27] Wojnarowicz, J., Chudoba, T., Gierlotka, S. & Lojkowski, W. Effect of microwave radiation power on the size of aggregates of ZnO NPS prepared using microwave solvothermal synthesis. Nanomaterials (Basel) **8** (2018) 343.
[28] Anwar, J. et al. Microwave Chemistry: Effect of ions on dielectric heating in microwave ovens. Arabian Journal of Chemistry **8** (2015) 100-104.
[29] Zakharov, N. A., Sentsov, M. Yu. & and Kuznetsov, N. T. Effect of microwave exposure on the morphology of calcium hydroxyapatite nanocrystals synthesized from aqueous solutions. Russian Journal of Inorganic Chemistry **62** (2017) 22-26.
[30] Eslami, H., Solati-Hashjin, M. & Tahriri, M. The comparison of powder characteristics and physicochemical, mechanical and biological properties between nanostructure ceramics of hydroxyapatite and fluoridated hydroxyapatite. Materials Science and Engineering C **29** (2009) 1387-1398.
[31] Barandehfard, F., Keyanpour-Rad, M., Hosseinnia, A., Kazemzadeh, S. M., Vaezi, M. R. & Hassanjani-Roshan, A. Sonochemical synthesis of hydroxyapatite and fluoroapatite nanosized bioceramics. Journal of Ceramic Processing Research **13** (2012) 437-440.

[32] Nikčević, I., Jokanović, V., Mitrić, M., Nedić, Z., Makovec, D., & Uskoković, D. Mechanochemical synthesis of nanostructured fluorapatite/fluorhydroxyapatite and carbonated fluorapatite/fluorhydroxyapatite. Journal of Solid-State Chemistry **177** (2004) 2565–2574.
[33] Hincke, M. T., Nys, Y., Gautron, J., Mann, K., Rodriguez-Navarro, A. B. & McKee, M. D. The eggshell: structure, composition, and mineralization. Frontiers in Bioscience **17** (2012) 1266-1280.
[34] Lin, S., Kiga, T., Wang, Y. & Nakayama, K. Energy analysis of $CaCO_3$ calcination with CO_2 capture. Energy Procedia **4** (2011) 356-361.
[35] Borkowski, L. et al. Fluorapatite ceramics for bone tissue regeneration: Synthesis, characterization, and assessment of biomedical potential. Materials Science & Engineering C **116** (2020) 111211.
[36] Lafon, J. P., Champion, E. & Bernache-Assolant, D. Processing of AB-type carbonated hydroxyapatite Ca_{10}-$x(PO_4)_6$-$x(CO_3)x(OH)_2$-x-$2y(CO_3)y$ ceramics with controlled composition. Journal of the European Ceramic Society **28** (2008) 139–147.
[37] Bulina, N. V., Makarova, S. V., Prosanov, I. Y., Vinokurova, O. B. & Lyakhov, N. Z. Structure and thermal stability of fluorhydroxyapatite and fluorapatite obtained by mechanochemical method. Journal of Solid State Chemistry **282** (2019) 121076.
[38] Zhao, J. *et al.* Solution combustion method for synthesis of nanostructured hydroxyapatite, fluorapatite and chlorapatite. Applied Surface Science **314** (2014) 1026-1033.
[39] Kee, C. C., Ismail, H. & Noor, A. F. M. Effect of synthesis technique and carbonate content on the crystallinity and morphology of carbonated hydroxyapatite. Journal of Material Science and Technology **29** (2013) 761-764.
[40] Safarzadeh, M. *et al.* Sintering behaviour of carbonated hydroxyapatiteprepared at different carbonate and phosphateratios. Boletin de Lasociedad Espanola de Ceramica Y Vidrio **59** (2020) 73-80.
[41] Rodriguez-Lorenzo, L. M., Hart, J. N. & Gross, H. A. Influence of fluorine in the synthesis of apatites. Synthesis of solid solutions of hydroxy-fluorapatite. Biomaterials **24** (2003) 3777–3785.